Available online at www.sciencedirect.com

ScienceDirect

IFAC PapersOnline CONFERENCE PAPER ARCHIVE

IFAC PapersOnLine 51-8 (2018) 120–125

Slug handling with a virtual harp based on nonlinear predictive control for a gravity separator ⋆

Christoph Josef Backi *,1 **Dinesh Krishnamoorthy** * **Sigurd Skogestad** *

* *Department of Chemical Engineering, Norwegian University of Science and Technology (NTNU), 7491 Trondheim, Norway (e-mail: {christoph.backi,dinesh.krishnamoorthy,sigurd.skogestad}@ntnu.no).*

Abstract: This paper presents a nonlinear model predictive control approach for a three-phase gravity separator model. The aim of the controller is to dampen slug-induced, oscillatory disturbances in the inflow to the gravity separator. This means that, despite the disturbance, the levels of water and oil as well as the pressure should be held at constant operational setpoints. Additionally, a second objective is to dampen the outflows of water, oil and gas and hence keep too large oscillations in flows from downstream equipment. Several constraints are added such as the height of the weir, maximal and minimal allowable levels and pressures as well as constraints on the outflows.

Keywords: Gravity separator, nonlinear model predictive control, slug handling, virtual harp

1. INTRODUCTION

In the oil- and gas-industry, the separation of phases such as gas, water and hydrocarbons (oil and condensate) from a well stream is crucial to obtain as pure single phase streams as possible. Thereby, often gravity separators are utilized as a first rough separation stage followed by a number of refining stages, for example hydrocyclones, gas scrubbers, gas flotation units and in special cases also membranes. After all these separation stages, the phases should be pure enough to preferably distribute them further by standard single phase pumps and compressors (oil and gas). In addition, disposal into the sea (water) or reinjection back into the reservoir (water and gas) are further options. This paper focuses on gravity separation devices, which are based on separation by gravitational forces and density differences between the respective dispersed and continuous phases (Arntzen, 2001; Bothamley, 2013). This means that water droplets dispersed in the oil-continuous phase will settle towards their bulk water-continuous phase whereas oil droplets dispersed in this water-continuous phase will rise to the oil-continuous phase.

Literature regarding control-oriented modeling of gravity separators is rather sparse. The main modeling efforts are towards CFD-based models investigating the flow patterns inside the separator and are mostly used for the purposes of design (optimization) or validation (Hansen, 2001; Laleh et al., 2012, 2013; Kharoua et al., 2013).

Gravity separators must be operated within specified limits making steady control of the state variables to nominal values necessary. These include for example limits on the gas pressure as well as on the water level, which should remain below the weir such that the water-continuous phase does not enter the outflow of the oil-continuous phase. Disturbances to the process can cause the state variables to leave these specified limits making steady control action necessary. Such disturbances can for instance be slug inflows, which express themselves in alternating oscillations in the inflows of gas and liquid. Riser-induced slugging has attracted the attention of researchers in recent decades and can be controlled by a large variety of (nonlinear) control methods (Jahanshahi and Skogestad, 2017; Jahanshahi et al., 2017; Jahanshahi and Skogestad, 2013). Furthermore, the installation of large volumes in the form of harp-style slug catchers can avoid excessive oscillatory behavior. In this work we concentrate on the case, where the slug controllers are either not implemented or only able to dampen the slug-induced oscillations insufficiently, and when harp-style slug catchers are not installed.

As the title says, we design a "virtual harp", which provides a similar effect like a harp-style slug catcher. It is based on the model predictive control (MPC) methodology to reduce oscillations in the outflows of gas, water and oil and at the same time keep the state variables (total liquid level, water level and pressure) at certain setpoints inside defined bounds. However, there exists a trade-off between dampening the slug-induced oscillations in the outflows and dampening the oscillations in the state variables. Therefore, the exact objective and hence tuning are very important tasks.

The remainder of this paper is structured as follows: Section 2 introduces the mathematical mode, which is the basis for controller design, while the controller itself is designed in Section 3. Section 4 presents simulation

⋆ This work was supported by the Norwegian Research Council under the project SUBPRO (Subsea production and processing)

[1] corresponding author

10.1016/j.ifacol.2018.06.365

results, whereas in Section 5 the paper is closed with some concluding remarks.

2. MATHEMATICAL MODEL

A schematic of the gravity separator is shown in Fig. 1. Basically, it is a long cylinder, where the multiphase inlet stream is fed into the separator at the left side. Due to turbulence, a first rough separation occurs in the inlet zone. For simplicity, we assume that the gas is completely flashed out of the liquid phases, meaning that no gas bubbles exist therein. Additionally, we assume that no liquid droplets can be found in the continuous gas phase. The active separation zone of length L follows the inlet zone, in which dispersed droplets settle or rise to their respective bulk phases due to density differences. Phenomena like for example breakage (big droplets break into smaller droplets) and coalescence (small droplets form a big droplet) are neglected, but are likely to occur. The gas, water and oil phases leave the separator in the outlet zone on the right hand size of the separator. More simplifying assumptions include an average velocity for the respective oil- and water-continuous layers including the dispersed droplets (no slip between droplets and continuous phase) as well as the absence of an emulsion (dense-packed) layer between these layers. Typically, in order to get a more even flow in gravity separators, flow-distribution baffles are added along the x-direction (not specifically shown here).

The focus in this paper is not on overall separation of the three phases, but for completeness our model also includes droplet calculations for oil in water and water in oil.

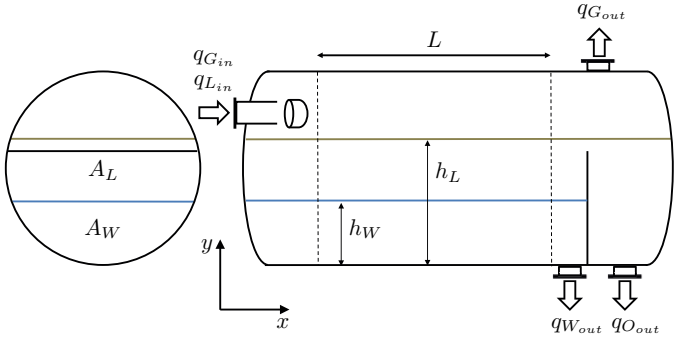

Fig. 1. Simplified schematic of the gravity separator with a cross-sectional view on the left-hand side

2.1 Differential part of the model

The mathematical model that is the basis for controller design in Section 3 was introduced in detail in Backi and Skogestad (2017a). The differential part of the model consists of three states, the overall liquid level h_L (oil plus water), the water level h_W and the gas pressure p.

Based on in- and outflow dynamics, the following differential equations are obtained for the water and liquid levels (Backi and Skogestad, 2017b)

$$\frac{dh_L}{dt} = \frac{dV_L}{dt}\frac{1}{2L\sqrt{h_L(2r-h_L)}}, \tag{1}$$

$$\frac{dh_W}{dt} = \frac{dV_W}{dt}\frac{1}{2L\sqrt{h_W(2r-h_W)}}, \tag{2}$$

with radius of the gravity separator vessel r and length of the active separation zone L . The changes of volumes for the liquid and water phases are given by the volumetric in- and outflow dynamics

$$\frac{dV_L}{dt} = q_{L,in} - q_{L,out} = q_{L,in} - q_{W,out} - q_{O,out}, \tag{3}$$

$$\begin{aligned}\frac{dV_W}{dt} &= q_{W,in} - q_{W,out} \\ &= q_{L,in}\left[\alpha\phi_w + (1-\alpha)(1-\phi_o)\right] - q_{W,out},\end{aligned} \tag{4}$$

where α is the water cut, q_i denote in- or outflows of either liquid (L), water (W) or oil (O), ϕ_w represents the fraction of inflowing water going into the water-continuous phase and ϕ_o defines the fraction of inflowing oil going into the oil-continuous phase. In (4), $\alpha\phi_w$ denotes the fraction of total inflowing water and $(1-\alpha)(1-\phi_o)$ represents the fraction of total inflowing oil, both into the water-continuous phase.

The pressure dynamics are derived from the ideal gas law assuming constant temperature and are scaled here for the unit [bar]

$$\frac{dp}{dt} = 10^{-5}\left[\frac{RT\frac{\rho_G}{M_G}\left(q_{G,in} - q_{G,out}\right) + 10^5 p\left(q_{L,in} - q_{L,out}\right)}{V_{Sep} - V_L}\right] \tag{5}$$

with volume of the active separation zone V_{Sep}, liquid volume

$$V_L = \frac{r^2 L}{2}\left[2\cos^{-1}\left(\frac{r-h_L}{r}\right) - \sin\left(2\cos^{-1}\left(\frac{r-h_L}{r}\right)\right)\right],$$

universal gas constant R, temperature T, density of gas ρ_G, molar mass of gas M_G and the in- and outflows of gas (G) and liquid (L), respectively.

The manipulated variables are the outflows of oil, water and gas, hence $\mathbf{u} = [q_{O,out}\ q_{W,out}\ q_{G,out}]^T$. Disturbance variables are the inflow of liquid $q_{L,in}$ (sum of the inflows of water and oil) and the inflow of gas $q_{G,in}$.

2.2 Algebraic part of the model

In addition to the differential part described above, the model consists of an algebraic part, which is constituted by droplet distribution calculations in the oil- and water-continuous phases in the active separation zone. Therefore, we define 10 droplet size classes and assume their diameters $d_i = \{50, 100, 150, \ldots, 500\}\mu$m with initial distributions $\mathbf{n^{O/W}} = 10^8\,[1\ 5\ 10\ 50\ 100\ 100\ 50\ 10\ 5\ 1]$, which is weighted by factors F_W (water droplets) and F_O (oil droplets) to regard for the fractions of inflowing water and oil to the respective phases. These assumptions imply that the droplet volumes for oil and water are alike $V_i^O = V_i^W = \frac{\pi}{6}d_i^3$.

For each droplet class i the vertical residence time t_{v_i} is compared to its horizontal residence time $t_h^{W/O}$. Latter is calculated by the length L divided by the horizontal velocities of the oil and water phases, which are given by the inflows of oil and water divided by the respective cross-sectional areas, $v_h^{W/O} = \frac{q_{O/W,in}}{A_{O/W}}$, hence

$$t_h^{W/O} = \frac{A_{O/W} L}{q_{O/W,in}} \tag{6}$$

with $A_O = A_L - A_W$ and $q_{O,in} = q_{L,in} - q_{W,in}$. The vertical residence time is based on Stokes' law giving a vertical velocity for each droplet size class i

$$v_{v_i} = \frac{g d_i^2 \left(\rho_d - \rho_c\right)}{18 \mu_c}, \tag{7}$$

where g is the gravitational acceleration, ρ_d and ρ_c are the densities of the dispersed and continuous phases, respectively, and μ_c indicates the dynamic viscosity of the continuous phase. If a droplet reaches the oil-water-interface, its respective volume is added to its bulk phase and subtracted from the phase it was dispersed in.

For oil droplets dispersed in the water-continuous phase the removed volume is calculated via Algorithm 1.

Algorithm 1 Calculation of droplet class positions and separated volume for oil droplets

for i = 1:10 **do**
  if $t_h^O < t_{v_i}^O$ **then**
    $z_i^O = t_h^O v_{v_i}^O$
  else
    $z_i^O = h_W$
  end if
  $V_i^{OoW} = n_i^O V_i^O \frac{z_i^O}{h_W}$
end for

with $\sum_{i=1}^{10} V_i^{OoW} = V^{OoW}$ and $t_{v_i}^O = \frac{h_W}{v_{v_i}^O}$.

In addition, for water droplets dispersed in the oil-continuous phase, the removed volume is calculated accordingly via Algorithm 2.

Algorithm 2 Calculation of droplet class positions and separated volume for water droplets

for i = 1:10 **do**
  if $t_h^W < t_{v_i}^W$ **then**
    $z_i^W = t_h^W v_{v_i}^W$
  else
    $z_i^W = h_O$
  end if
  $V_i^{WoO} = n_i^W V_i^W \frac{z_i^W}{h_O}$
end for

where $\sum_{i=1}^{10} V_i^{WoO} = V^{WoO}$ and $t_{v_i}^W = \frac{h_O}{v_{v_i}^W}$ with $h_O = h_L - h_W$.

The positions of droplet classes $\mathbf{z} = \begin{bmatrix} \mathbf{z^O} & \mathbf{z^W} \end{bmatrix}$ represents the vector of algebraic variables.

The factors F_W and F_O are calculated as follows

$$F_W = t_{h,inlet}^O \left[\alpha \left(1 - \phi_w\right)\right] q_{L,in} \frac{1}{V_W},$$

$$F_O = t_{h,inlet}^W \left[\left(1 - \alpha\right)\left(1 - \phi_o\right)\right] q_{L,in} \frac{1}{V_O},$$

where $t_{h,inlet}^O$ and $t_{h,inlet}^W$ are the residence times of droplets in the inlet zone of the separator in the respective water- and oil-continuous phases, and $V_O = \sum_{i=1}^{10} n_i V_i^O$ as well as $V_W = \sum_{i=1}^{10} n_i^W V_i^W$.

The algorithm as listed above is not implementable as such. In fact, the if-else-end statements switch between two cases, namely if the horizontal residence time is smaller or equal/larger than the vertical residence times for each droplet class i. The optimization algorithm relies on a continuous formulation of the algorithm and its implementation is achieved by applying approximations based on an arctan-function with a steep gradient around a switching argument Δt representing the difference in residence times. Details are presented in Appendix A.

2.3 Maximization of separation efficiency

An investigation for maximizing the separation efficiency in the given separator model had the objective to maximize the outflows of oil from the water-continuous phase and water from the oil-continuous phase. Thereby, the water level and hence the horizontal and vertical residence times of droplets in the respective phases were subject to changes at a constantly held overall liquid level. Since both the initial distributions and the horizontal and vertical velocities are depending on the very same variable, i.e. levels of water and oil, the optimizer depending on their weights in the cost function will prefer either cleaner water or cleaner oil. This means that either the water level will be as high as possible or zero. In the following investigation we will therefore concentrate on the case favoring cleaner water and define the setpoint of water just below the weir.

3. CONTROLLER DESIGN

In order to dampen out slugging inflows and reduce their effect on the state variables as well as on the outflows of the gravity separator, we design a nonlinear model predictive controller. Thereby, the state variables should be kept at or close to desired setpoints and between safety-related limits. In addition, the variances of the inflows should not propagate through to the outflows, meaning that the gravity separator acts a slug tank and protects downstream equipment from too large oscillations of gas, water and oil. This is important since e.g. hydrocyclones do not tolerate large fluctuations in inflows with respect to separation efficiency and optimal operation. There exists a trade-off between oscillation reduction in the state and the manipulated variables.

In this work, we use a nonlinear model predictive control strategy to achieve the objective of balancing the fluctuations between the state and the manipulated variables. Before the MPC problem can be formulated, the optimal control problem is first discretized into a finite dimensional nonlinear optimization problem divided into N elements such that each interval is in $[t_k, t_{k+1}]$ for all $k \in \{1, \ldots, N\}$. A low order direct collocation scheme is used to provide a polynomial approximation of the system trajectories for each time interval $[t_k, t_{k+1}]$. In this work we use a third order Radau collocation scheme for the polynomial approximation. The resulting discrete version of the DAE model in sections 2.1 and 2.2 is represented as

$$\begin{aligned} \mathbf{x}_{k+1} &= \mathbf{f}(\mathbf{x}_k, \mathbf{z}_k, \mathbf{u}_k) \\ \mathbf{z}_k &= \mathbf{g}(\mathbf{x}_k, \mathbf{u}_k) \end{aligned} \tag{8}$$

where $\mathbf{x}_k$ represents the differential states (from Section 2.1) at time step k, $\mathbf{z}_k$ represents the algebraic states (from Section 2.2) and $\mathbf{u}_k$ denotes the control inputs (manipulated variables). Once the system is discretized, the nonlinear economic MPC problem can be formulated as

$$\begin{aligned} &\min\ J_{\text{states}} + J_{\text{outflows}} && \text{(9a)}\\ &\text{s.t.}\quad h_{W_k} \leq h_{\text{weir}} && \text{(9b)}\\ &\quad \mathbf{x}_{k+1} = \mathbf{f}(\mathbf{x}_k, \mathbf{z}_k, \mathbf{u}_k) && \text{(9c)}\\ &\quad \mathbf{z}_k = \mathbf{g}(\mathbf{x}_k, \mathbf{u}_k) && \text{(9d)}\\ &\quad \mathbf{x}_{min} \leq \mathbf{x}_k \leq \mathbf{x}_{max} && \text{(9e)}\\ &\quad \mathbf{u}_{min} \leq \mathbf{u}_k \leq \mathbf{u}_{max} && \text{(9f)}\\ &\quad \mathbf{x}_0 = \mathbf{x}_{\text{init}} && \text{(9g)}\\ &\forall k \in \{1, \ldots, N\} \end{aligned}$$

with the state setpoint tracking term

$$J_{\text{states}} = \sum_{k=1}^{N} \omega_{h_L} \left\| h_{L_k} - h_{L_k}^{sp} \right\|^2 + \omega_{h_W} \left\| h_{W_k} - h_{W_k}^{sp} \right\|^2 + \omega_p \left\| p_k - p_k^{sp} \right\|^2$$

and the term penalizing changes in the manipulated variables

$$\begin{aligned} J_{\text{outflows}} = \sum_{k=1}^{N} &\omega_{q_{O,out}} \left\| q_{O,out_k} - q_{O,out_{k-1}} \right\|^2 \\ &+ \omega_{q_{W,out}} \left\| q_{W,out_k} - q_{W,out_{k-1}} \right\|^2 \\ &+ \omega_{q_{G,out}} \left\| q_{G,out_k} - q_{G,out_{k-1}} \right\|^2. \end{aligned}$$

Furthermore, the objective function comprises of the constraint (9b), which enforces the water level to remain below the weir plate h_{weir}. This prevents the water-continuous phase to enter the oil-continuous outflow. In addition, upper and lower bounds are also enforced for the states and the control inputs in (9e) and (9f), respectively. We assume that the liquid level, water level and the separator pressures are measured. At each iteration, the initial conditions for the states are enforced in (9g).

The dynamic optimization problem is setup as a nonlinear programming problem in CasADi v3.0.1-rc1 (Andersson, 2013). The resulting NLP problem is then solved using IPOPT version 3.12.2 (Wächter and Biegler, 2006) running with a mumps linear solver. The plant simulator is solved with an ode15s solver. We simulate 600 MPC iterations with a sample time of $\Delta t = 1$ s. The prediction horizon of the NMPC controller is set to 20 s. The weights in the objective function are chosen as shown in Table 1. The NMPC problem is initialized with steady state values for liquid inflow of $q_{L,in} = 0.59$ m^3 s^{-1} and gas inflow $q_{G,in} = 0.456$ m^3 s^{-1} and the corresponding states with $h_W = 1.9$ m, $h_L = 2.3$ m and $p = 68.7$ bar. The weir height is set to $h_{\text{weir}} = 2$ m. The setpoint for water is $h_W^{sp} = 1.9$ m, that for the overall liquid level $h_L^{sp} = 2.5$ m (to have some reasonable buffer volume above the liquid level), and for the pressure $p^{sp} = 68.7$ bar. Most parameters are taken from Laleh et al. (2012) and the ones not listed here are summarized in Appendix B.

4. SIMULATIONS

This Section presents simulation results for two cases of severe slugging flows entering the gravity separator:

Table 1. Weights used in the NMPC problem.

weight	value	weight	value
ω_{h_L}	1	$\omega_{q_{O,out}}$	50
ω_{h_W}	1	$\omega_{q_{W,out}}$	10
ω_p	1	$\omega_{q_{G,out}}$	50

1.) Production from one well with only one sinusoidal slugging frequency, which oscillates around a nominal value of $q_{L,in} = 0.59$ m^3 s^{-1} and $q_{G,in} = 0.456$ m^3 s^{-1}.
2.) Production from three wells with three sinusoidal slugging frequencies, where each is weighted differently. Here, the main weight has been put on the higher-frequent oscillations, where all sinusoidals oscillated around the same nominal values as mentioned under point 1.) above

The two different cases are demonstrated in Fig. 2, where the two different characters of the slugging inflows to the gravity separator become apparent.

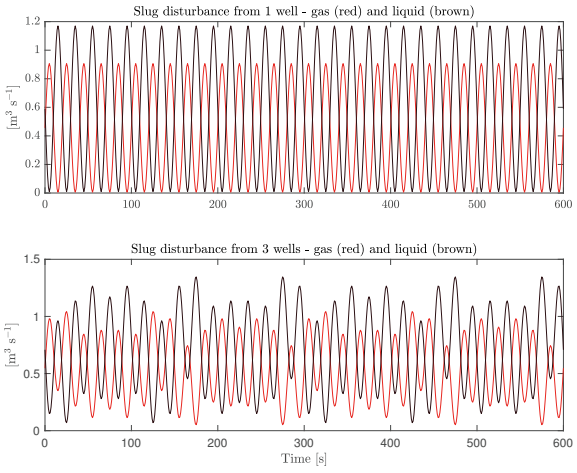

Fig. 2. Slugging inflows of liquid and gas to the separator

In the subsequent studies, we compare two different ways of MPC implementation. The first one assumed a constant disturbance in the prediction horizon, whereas for the second one the expected future disturbances were included in the prediction horizon.

4.1 Case 1 - Production from one well

Fig. 3 presents the simulation results for production from one well with constant disturbance in the prediction horizon. It can be seen that stabilization of the pressure and water level is quite good with the cost that the respective outflows on the right hand side oscillate quite heavily. In contrary, the oil level oscillates more heavily around its nominal value compared to the water level and gas pressure, however, its outflow (black plot) is less noisy compared to the the outflows of water and gas.

In Fig. 4, the same simulation case as presented above is demonstrated, however, this time with a time-varying disturbance anticipating the slug also in the prediction horizon. What becomes clear directly is the reduced oscillatory behavior for the outflows, whereas the performance

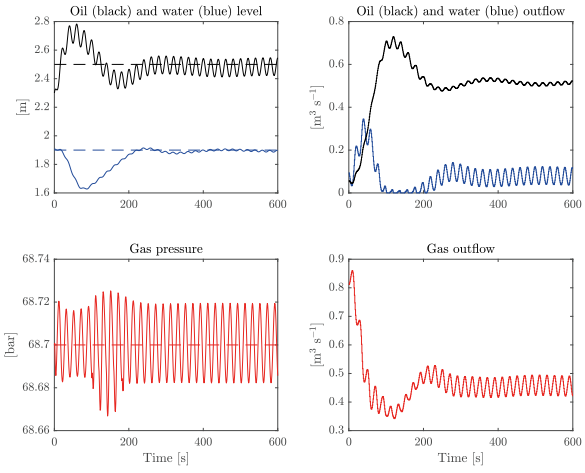

Fig. 3. Case 1 - state variables and manipulated variables for constant disturbance in the prediction horizon

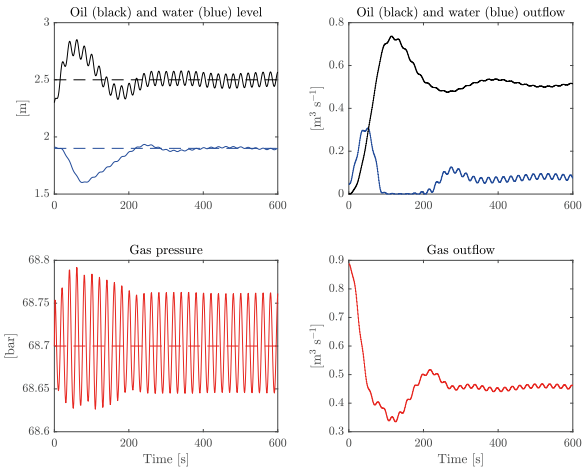

Fig. 4. Case 1 - state variables and manipulated variables for time-varying disturbance in the prediction horizon

with respect to setpoint tracking does not change much compared to before.

4.2 Case 2 - Production from three wells

In Fig. 5, simulations for the production from three wells with constant disturbance in the prediction horizon are shown. Comparing this case to the cases presented in Section 4.1, the heavier oscillations in the disturbance can clearly be seen in the water and oil levels, however performance for pressure setpoint tracking is the same as before. The outflows show a more noisy behavior and seem more influenced by low-frequent rather than high-frequent slugs.

Fig. 6 presents the same case as above, but again with a time-varying disturbance in the prediction horizon. Like for the case in Fig. 4, a clear reduction in oscillations can be seen for all outflows. Setpoint tracking for the state variables shows about the same performance as in Fig. 5 and hence the same trend as in Section 4.1 is identifiable.

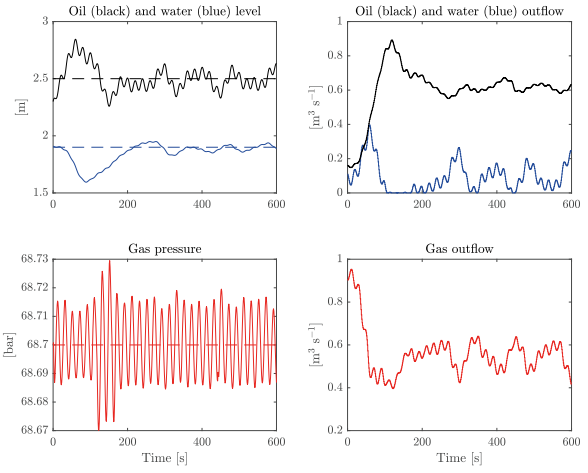

Fig. 5. Case 2 - state variables and manipulated variables for constant disturbance in the prediction horizon

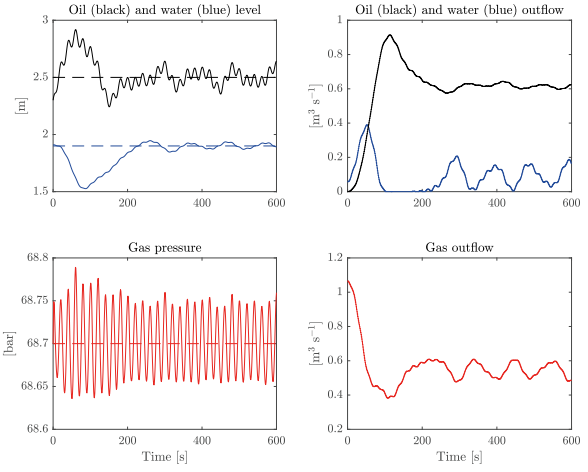

Fig. 6. Case 2 - state variables and manipulated variables for time-varying disturbance in the prediction horizon

4.3 Comparison

In Fig. 7, the cost functions for all presented cases are shown. The top plot shows the case for production from one well, whereas the bottom plot demonstrates production from three wells. What is apparent is the better performance for simulations with anticipated sinusoidal disturbances in the predictions horizon (blue plots) compared to the cases with constant disturbances (red plots).

5. CONCLUDING REMARKS

In this paper we presented a nonlinear model predictive control scheme for the minimization of the effect of slugging inflow disturbances on the state and the manipulated variables. Thereby, there exists a trade-off between the reduction in oscillations for the state variables and the manipulated variables. The model that was used for controller design is a differential algebraic equation model with 3 differential states defining the dynamic variables liquid level, water level and gas pressure as well as 20 algebraic

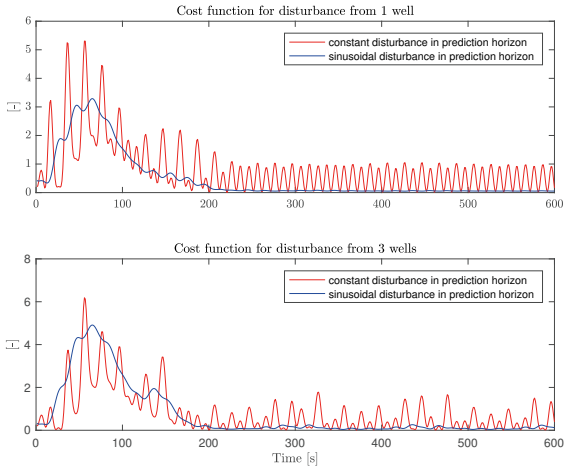

Fig. 7. Comparison of the cost function values for simulation cases 1 and 2

states characterizing the positions of droplet size classes at the end of the active separation zone. We defined 10 size classes for oil droplets and water droplets, respectively.

The results show that the controller is able to maintain the pressure as well as the oil and water levels at their desired setpoints and reduce the effect of the disturbances on the outflows as well. We presented two different kinds of disturbances as well as two solution strategies. From the simulations it became apparent that for both cases the solution strategy with non-constant, time-varying disturbances over the prediction horizon was superior.

This work merely presents a proof of concept and hence computational times are not reported. However, we are aware that the aspect of real-time applicability is of high significance for MPC implementations. For completeness, we used a quite detailed model with droplet calculations for oil in water and water in oil. However, in order to reduce computational time, using simpler, linear models could be an option.

REFERENCES

Andersson, J. (2013). *A general-purpose software framework for dynamic optimization*. PhD thesis, KU Leuven.

Arntzen, R. (2001). *Gravity Separator Revamping*. Ph.D. thesis, Norwegian University of Science and Technology, Trondheim, Norway.

Backi, C.J. and Skogestad, S. (2017a). A simple dynamic gravity separator model for separation efficiency evaluation incorporating level and pressure control. In *Proceedings of the 2017 American Control Conference*. Seattle, WA, USA.

Backi, C.J. and Skogestad, S. (2017b). Virtual inflow monitoring for a three phase gravity separator. In *Proceedings of the 1st IEEE Conference on Control Technology and Applications*. Kohala Coast, HI, USA.

Bothamley, M. (2013). Gas/Liquid Separators - Quantifying Separation Performance - Parts 1–3. *Oil and Gas Facilities*, 2(4,5,6), 21–29, 35–47, 34–47.

Hansen, E.W.M. (2001). Phenomelogical Modeling and Simulation of Fluid Flow and Separation Behaviour in Offshore Gravity Separators. In *Proceedings of the 2001 Pressure Vessel and Piping Conference*, volume 431, 23–29. Atlanta, GA, USA.

Jahanshahi, E., Backi, C.J., and Skogestad, S. (2017). Anti-slug control based on a virtual flow measurement. *Flow Measurement and Instrumentation*, 53, 299–307.

Jahanshahi, E. and Skogestad, S. (2013). Closed-loop model identification and PID/PI tuning for robust anti-slug control. *IFAC Proceedings Volumes*, 46(32), 233–240.

Jahanshahi, E. and Skogestad, S. (2017). Nonlinear control solutions to prevent slugging flow in offshore oil production. *Journal of Process Control*, 54, 138–151.

Kharoua, N., Khezzar, L., and Saadawi, H. (2013). CFD Modelling of a Horizontal Three-Phase Separator: A Population Balance Approach. *American Journal of Fluid Dynamics*, 3(4), 101–118.

Laleh, A.P., Svrcek, W.Y., and Monnery, W.D. (2012). Computational Fluid Dynamics-Based Study of an Oilfield Separator - Part I: A Realistic Simulation. *Oil and Gas Facilities*, 1(6), 57–68.

Laleh, A.P., Svrcek, W.Y., and Monnery, W.D. (2013). Computational Fluid Dynamics-Based Study of an Oilfield Separator - Part II: An Optimum Design. *Oil and Gas Facilities*, 2(1), 52–59.

Wächter, A. and Biegler, L.T. (2006). On the implementation of an interior-point filter line-search algorithm for large-scale nonlinear programming. *Mathematical Programming*, 106(1), 25–57.

Appendix A. ARCTAN APPROXIMATIONS

The switching argument Δt_i together with the arctan-function $\zeta_i(\Delta t_i)$

$$\Delta t_i = t_h^{W/O} - t_{v_i}^{O/W},$$
$$\zeta_i(\Delta t_i) = \frac{1}{\pi}\left(\arctan\left(1000\pi\Delta t_i\right) + \frac{\pi}{2}\right),$$

are used to calculate the positions $z_i^{O/W}$ of oil and water droplets at the end of the active separation zone

$$z_i^{O/W} = \zeta_i(\Delta t_i)h_{W/O} + (1-\zeta_i(\Delta t_i))\left(L\frac{v_{v_i}^{O/W}}{v_h^{W/O}}\right).$$

The function switches between the cases if a droplet size class i hits the interface, meaning $\zeta_i(\Delta t_i) = 1$ or if it remains dispersed, as for $\zeta_i(\Delta t_i) = 0$.

Appendix B. PARAMETERS

g	gravitational acceleration	≈ 9.8 m s^{-1}
L	Length (active separation zone)	10 m
M_G	Molar mass of the gas	0.01604 kg mol^{-1}
r	Radius of the separator	1.65 m
R	Universal gas constant	8.314 $\frac{\text{kg m}^2}{\text{s}^2\ \text{mol K}}$
T	Temperature	328.5 K
V_{Sep}	Volume (active separation zone)	85.53 m^3
α	Water cut of the liquid inflow	0.135
μ_O	Dynamic viscosity oil	0.001 kg (s m)$^{-1}$
μ_W	Dynamic viscosity water	0.0005 kg (s m)$^{-1}$
ρ_G	Density of gas	49.7 kg m^{-3}
ρ_O	Density of oil	831.5 kg m^{-3}
ρ_W	Density of water	1030 kg m^{-3}
ϕ_w	Initial water to water fraction	0.1
ϕ_o	Initial oil to oil fraction	0.9